JOURNAL OF APPLIED ELECTROCHEMISTRY 17 (1987) 914–924

Chromium–titanium–antimony oxide composite anodes: electro-organic oxidations

F. BECK, H. SCHULZ

University of Duisburg GH, FB6-Elektrochemie, Lotharstr. 1, D4100 Duisburg 1, Federal Republic of Germany

Received 23 September 1986; revised 2 December 1986

An activated titanium electrode with an oxide layer, composed of a mixture of Cr_2O_3, TiO_2 and Sb_2O_3 (optimal mole ratio chromium : titanium : antimony about 2 : 1 : 1) has been fabricated by thermal decomposition of the chlorides on a titanium substrate at 650° C. The black-green layer adheres well and has a thickness in the order of micrometres. Its structure is explained using a pore model, based on SEM, AES and electrochemical results. Service life time of electrodes in 1 M H_2SO_4 for oxidation of isopropanol in terms of the turn over factor of Cr_2O_3 is between 100 and 400.

Preparative electro-organic oxidations of isopropanol, tetrahydrofuran and ethylbenzene have been performed with current densities of 0.5 to 5 mA cm^{-2}. The current efficiencies for the main products, acetone, γ-butyrolactone and acetophenone are 100, 53 and 20%, respectively. These results parallel those of the homogeneous oxidation with chromic acid in solution.

1. Introduction

Chromic acid has been widely used for the selective chemical oxidation of organic compounds, at least on the laboratory scale [1–5]. However, industrial application of this interesting reaction technique suffers from the following disadvantages:

(i) high cost of chromic acid,

(ii) severe toxicity of Cr(VI) compounds,

(iii) difficult separation of spent oxidant (Cr(III) sulphate) from the reaction mixture,

(iv) recycling Cr(III) to Cr(VI) (chemically or electrochemically) leads to a troublesome two-step process.

Nevertheless, indirect electrochemical oxidation with chromic acid is the only industrial process in this field so far developed [6–8]. The optimum anode material is Pb/PbO_2, cf. [9].

An early proposal simplifies the reaction technique in dissolving small amounts of Cr(III) salts in the electrolyte. Cr^{3+} ions are oxidized at the anode, thus acting as a redox mediator [10]. The chemical step proceeds in a reaction layer in front of the anode, and Cr^{3+} ions are regenerated as the electroactive species. Recently, we have proposed to transform this homogeneous redox catalysis into a heterogeneous one. A ceramic layer of Cr_2O_3 (mixed with TiO_2) on titanium base metal was fabricated [11] and investigated electrochemically [12–14]. Beer's invention of activated titanium electrodes [15, 16] was the starting point of our own development. In contrast to Cr_2O_3 on chromium or chromium steels [17], the Ti/Cr_2O_3, TiO_2 system worked essentially as a surface-fixed redox system, and turn over factors (TOF) of several hundred could be realized. The last two techniques, homogeneous and heterogeneous redox catalyses, are 'one step in cell processes', thus being superior from an engineering point of view. Anodic oxidation with Ti/Cr_2O_3, TiO_2 seems to be the most simple way to achieve chromic acid oxidations. We report here the fabrication of preparative electrodes of good stability and their employment in three different organic electrosyntheses.

2. Experimental details

2.1. *Fabrication of activated titanium anodes*

Titanium sheet or expanded sheet, 1 mm thick (Contimet 35, Thyssen Edelstahlwerke AG,

0021–891X/87 $03.00 + .12

Krefeld), was used in all cases. The material contains typically: 0.25 wt % Fe, 0.18 wt % O, 0.08 wt % C, 0.05 wt % N and 0.6 wt % others. After cleaning and degreasing the titanium surface by wet brushing with scrubbing powder, an etching step in 10% oxalic acid at 95° C for 1 h (in some cases 15 min) was performed. Etching in 20% HCl at 95° C for 15–60 min led to almost the same results.

For electrochemical measurements a strip of pretreated titanium, 60 × 10 × 1 mm, was activated on one side by the following method. A 50-μl sample of an activation solution (see below) was spread evenly over 4.5 cm^2 of the strip. Due to good surface roughening after the etching procedure, the liquid film adhered well. After drying (at 80° C for 10 min) the electrode was fired at 650° C for 5 min in a muffle furnace in the presence of air. This 'activation cycle', i.e. application of activation solution, drying, firing, was repeated twice. The number of activation cycles, Z_a, was therefore equal to 3.

The activation solution contained 0.5 wt % chromium (as $CrCl_3 \cdot 3H_2O$) and 0.25 wt % titanium (as $Ti(OBu)_4$, titanium n-butanolate) in isopropanol. The density, s, of the solution was equal to 0.79. The solution had an intensive green colour and was stable. The ester hydrolysed quantitatively during the drying step; thus losses due to evaporation in the firing step were omitted [18]. The Ti/Cr_2O_3, TiO_2 electrode, termed 'the standard binary oxide anode' had a surface concentration, n_A, equal to 2.52 μmol chromium per cm^2 ≡ 1.31 g chromium per m^2. The mole ratio of chromium : titanium was 2 : 1.08. The theoretical charge, $Q_{A,O}$, for a three-electron process is equal to 0.73 C cm^{-2}. In some cases, 66.7 μl of the activation solution was spread evenly over 7.4 cm^2 titanium. After three activation cycles, n_A = 2.05 μmol chromium per cm^2 and $Q_{A,O}$ = 0.60 C cm^{-2}. Electrode design and further experimental details are described elsewhere [11, 19].

Improved stability was obtained by adding 0.54 wt % antimony (as $SbCl_5$) to the activation solutions. All other parameters remained the same. The mole ratio of chromium : titanium : antimony was 2 : 1.08 : 0.92. This Ti/Cr_2O_3, TiO_2, Sb_2O_4 electrode is termed 'the standard ternary oxide anode'.

For preparative electrolysis, a larger, cylindrical titanium electrode, 60 mm high and 80 mm in diameter, made from expanded mesh (nine meshes per cm^2), was activated, following the same procedures as described previously with the following important variation. The activation solution was sprayed (from a glass atomizer) onto the cylinder standing on a hand driven, slowly rotating disc in a 'spraying cabin' made from a can. The titanium was preheated to 120° C. After drying and before firing (7 min at 650° C), the procedure was repeated once. From the mass gain this type of application correlated with one activation cycle as described above.

2.2. *Electrochemical conditions*

Electrochemical measurements were mostly carried out by slow cyclic voltammetry. The standard voltage scan rate was 5 mV s^{-1}. Conventional three-electrode arrangements in undivided cells were used. The reference electrode was $Hg/Hg_2SO_4/1\,M\ H_2SO_4$, and the potential, U_S, was + 674 vs SHE. The electrolyte was 1 M H_2SO_4 (H_2SO_4 analytical grade, doubly distilled water). The organic compounds were distilled and had a concentration of 1 M. Temperature was 25° C and solutions were not deaerated.

Preparative anodic oxidations were run in a 500-ml cylindrical cell with cooling jacket and planar ground joint. The anode area was 300 cm^2. The cathode was a wire of stainless steel or platinum, arranged coaxially, with an area of 1.8 cm^2. In this way, reduction of organics was substantially circumvented in this 'quasi divided cell' [20, 21]. The solution was stirred magnetically. The scale of preparative runs was 0.1–0.5 mol. Due to low current densities (0.5–5 mA cm^{-2}) only a slight amount of water cooling was necessary. The conversion of starting materials was 20–60%.

2.3. *Analytical procedures*

Most of the product analysis was performed with high performance liquid chromatography (HPCL). One important advantage of this technique is the possibility of direct determination of

products even in strongly acid solutions. Eluents were H_2SO_4, pH 1.7, or H_2O/methanol 2/1 or 3/1 (v/v). A fuller description of apparatus and procedures is given in [20, 21].

3. Results and discussion

3.1. *Structure and texture of electrode material*

The binary oxide electrodes Ti/Cr_2O_3, TiO_2 had a dark green colour, the ternary oxide electrodes with additional Sb_2O_4 were nearly black. The adherence of the thin oxide layers was excellent in both cases. The thermal decomposition of $CrCl_3$ in air to Cr_2O_3 as the most stable chromium oxide has been known for a long time, cf. [11]. Even CrO_3 decomposes thermally to yield Cr_2O_3 [22]. CrO_2 decomposes at $t > 400°$ C (in air) to Cr_2O_3 [23]. It is not surprising, therefore, that α-escolaite (Cr_2O_3) is the only oxide modification which has been found by our X-ray diffraction measurements [11]. TiO_2 does not crystallize in the presence of Cr_2O_3; it is amorphous and serves as a 'binder' for the chromium oxide. Only the thermal decomposition of $Ti(OBu)_4$ in the absence of $CrCl_3$ yields crystalline TiO_2 in the anatase form [24]. Little evaporation of the ester occurs [18]. The systems containing antimony have broader chromium X-ray diffraction lines (from Cr_2O_3) and titanium lines (from the base metal). The most intensive new lines are at $d = 3.232$ and $d = 3.008$ Å, corresponding to β- and α-Sb_2O_4. Sb_2O_5 must be excluded due to thermal decomposition at 380° C. Pure antimony oxides also yield Sb_2O_4 on firing in air, but only at temperatures above 700° C [25].

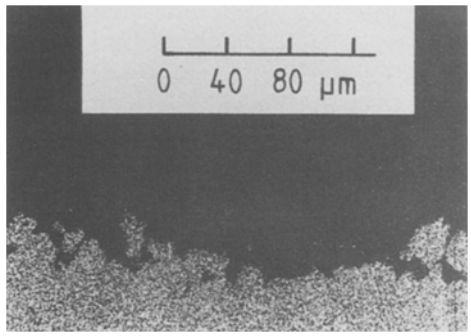

Fig. 2. SEM photograph of a slanting cross-section (α = 8°) of a standard Ti/Cr_2O_3, TiO_2 electrode. Energy dispersive analysis for chromium reveals its presence in the oxide layer (bottom). The measurement was provided by Dr U. Stroeder, Heraeus Co.

The thickness of standard oxide layers is about 0.7 µm. As the conductivity of α-Cr_2O_3 at room temperature is only in the order of 10^{-5} S cm^{-1} [26–29], the oxide film must be considered to be non-porous for electrical reasons. The texture of the activated titanium anode is revealed by SEM techniques, cf. Fig. 1. After etching, a highly disordered surface texture was developed. Activation of such an etched electrode leads to a filling of the 'valleys' with the oxide mixture (which itself has a cloddy structure), while the summits remain virtually uncovered. An SEM micrograph of the electrode along a slanting cross-section is in accordance with this view (Fig. 2). The presence of chromium in the oxide layer was detected by energy dispersive analysis. The excellent interlocking

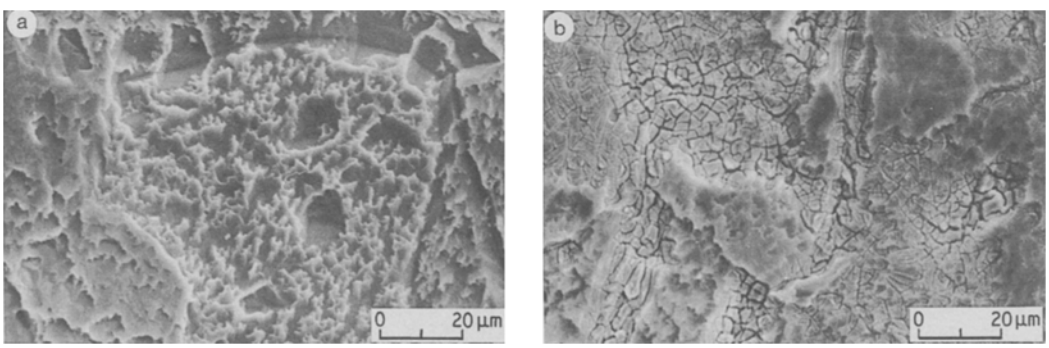

Fig. 1. SEM photographs of titanium electrodes. (a) After etching in 10% oxalic acid for 60 min at 95° C. (b) After application of a standard binary oxide layer ($d = 0.7$ µm) Ti/Cr_2O_3, TiO_2.

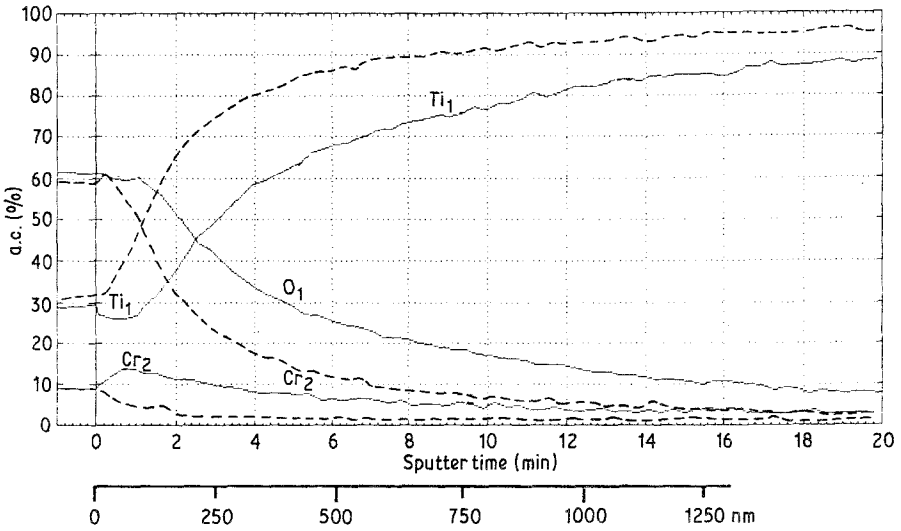

Fig. 3. Auger electron spectroscopy, 5 kV, 1 μA, sputter profiles for chromium, titanium and oxygen. Sputter rate, 80 nm min^{-1} (Ta_2O_5 reference). ——, Standard Ti/Cr_2O_3, TiO_2 ($d \approx 0.7\,\mu$m), original curve. – – –, Averaged curve drawn after potentiodynamic stripping of sample 1; 5 mV. The measurement was provided by Dr Hantsche, BAM, Berlin.

between the layer and the etched metal is clearly demonstrated and accounts for the good adhesion.

A third confirmation of the complicated nature of the electrode surface was possible with the help of Auger electron spectroscopy. The sputter profiles for the elements O, Ti and Cr are given in Fig. 3. At the surface, an inverted ratio of titanium : chromium of 2 : 1 is found instead of the analytical ratio of $\approx 1:2$. This is due to the presence of titanium 'mountains' penetrating the oxide layers. The dashed curve shows, in addition, that anodic stripping of chromium is not quantitatively due to a passivation of the Cr_2O_3 surface (see below).

Experimental evidence leads to a model of electrode texture which is summarized in Fig. 4. The oxide layer is porous. In addition, pores, gaps between the clods as shown in Fig. 1b may play an important role. The oxide layer does not contact the titanium metal directly, but rather through a thin TiO_2 film doped with Cr_2O_3 [11]. The pores are filled with electrolyte which has a much higher conductivity. Thus, the electrochemical reaction concentrates at the bottom of the pores [12]. This finally leads to an undermining of the crystallites upon anodic dissolution and explains its non-quantitative dissolution [11].

3.2. *Improvement of anode service life*

3.2.1. Binary oxides. According to our kinetic model [11, 12, 14], electrode service life is limited by dissolution of surface-bound CrO_3 through a hydration step:

$$(CrO_3)_s + H_2O \xrightarrow{k_{diss}} HCrO_4^- + H^+ \quad (1)$$

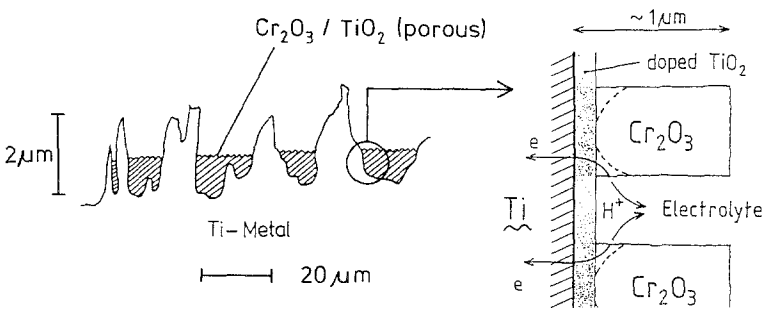

Fig. 4. Model of the porous layer of a Cr_2O_3, TiO_2 oxide on etched titanium base metal.

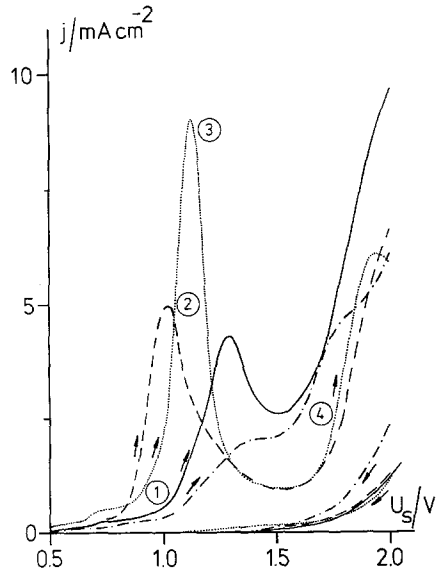

Fig. 5. Current–voltage curves for Ti/Cr_2O_3, TiO_2 electrodes in 1 M H_2SO_4 (T_A = 650° C, t_A = 3 × 5 min, Z_a = 3, $Q_{A,O}$ = 0.60 C cm^{-2}) v_S = 5 mV s^{-1}. Variation of chromium : titanium atomic ratio in the oxide layer: – – –, 2 : 0; · · · ·, 2 : 1.08; ——, 2 : 2; – · – · –, 2 : 3.

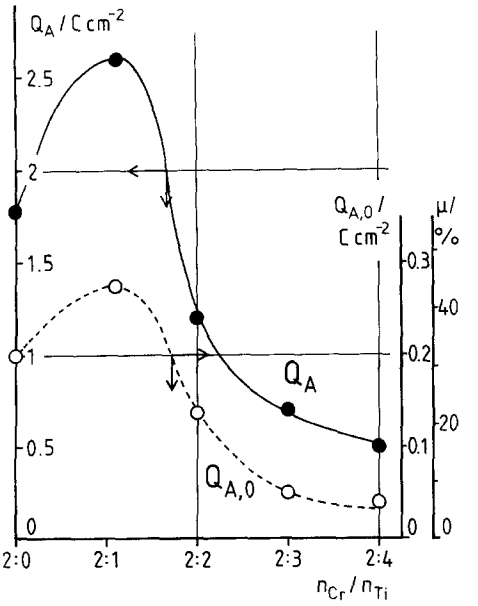

Fig. 6. Electrode service life (via potentiodynamic measurements) as a function of chromium : titanium atomic ratio for Ti/Cr_2O_3, TiO_2 anodes. o——o, Basic curve in 1 M H_2SO_4. ●——●, Curve for 1 M H_2SO_4/1 M isopropanol. $Q_{A,O}$ and Q_A are from the integrated curves of Fig. 5 and Fig. 7, respectively.

where $(CrO_3)_s$ is the CrO_3 species at the surface. This reaction competes with the chemical step of the redox catalysis cycle, leading to the wanted product, e.g. in the case of isopropanol:

$$2(CrO_3)_s + 3Me_2CHOH \xrightarrow{k} (Cr_2O_3)_s + 3Me_2CO + 3H_2O \quad (2)$$

The kinetic consequences of this mechanism are discussed elsewhere [12]. One possible way of improving the anode life is to adjust the optimal concentration of the 'binder' TiO_2. Fig. 5 shows a strong effect of the chromium : titanium ratio on the current voltage behaviour. The optimum ratio is 2 : 1, as in the standard mixture. The current–voltage curve goes through a maximum and rises again at very positive potentials. The qualitative interpretation of the sections is as follows.

(1) Anodic oxidation of $(Cr_2O_3)_s$ to CrO_3;
(2) increasing depletion of $(Cr_2O_3)_s$;
(3) passivation of $(Cr_2O_3)_s$ by CrO_3 filming;
(4) O_2 evolution on doped TiO_2 at the bottom of the pores. This will be quantitatively discussed in a forthcoming paper [30].

High concentrations of TiO_2 lead to distorted current–voltage behaviour and to much lower chromium utilization, μ, in the basic curve, cf. Fig. 6. This may be due to partial coverage of Cr_2O_3 by amorphous TiO_2 films.

If current–voltage curves are measured in the presence of an oxidizable substrate, e.g. isopropanol, a typical current amplification occurs

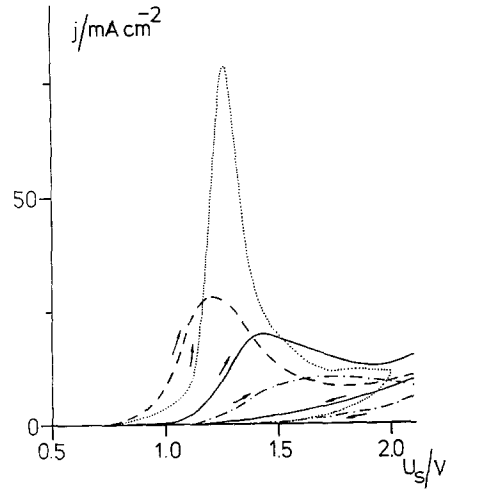

Fig. 7. Current–voltage curves for standard Ti/Cr_2O_3, TiO_2 electrodes in 1 M H_2SO_4/1 M isopropanol, v_S = 5 mV s^{-1}. Variation of chromium : titanium atomic ratio in the oxide layer: – – –, 2 : 0; · · · ·, 2 : 1.08; ——, 2 : 2; – · – · –, 2 : 3.

Table 1. Service life time of standard Ti/Cr_2O_3, TiO_2 anodes with 1 M H_2SO_4/1 M isopropanol

Measurement	Q_A ($C\,cm^{-2}$)	TOF_{pract} ($Q_{A,O} = 0.30\,C\,cm^{-2}$)
Potentiodynamic		
$5\,mV\,s^{-1}$, cf. Fig. 6	2.6	8.7
Galvanostatic		
$j = 20\,mA\,cm^{-2}$	10.4	35
$j = 2\,mA\,cm^{-2}$	19.4	65
$j = 0.2\,mA\,cm^{-2}$	38	127

due to heterogeneous redox catalysis (Fig. 7). The curves are similar to those of Fig. 5, but they are amplified by about one order of magnitude. The practical TOF (Table 1) is about 9 (for a definition of TOF_{pract} see Section 4).

The service life time, τ, of the electrodes depends strongly on current density, j. In accordance with our kinetic model it has been found that the surface specific charge, Q_A, which has been measured galvanostatically in the region of 0.1–20 mA cm^{-2}, decreases sharply with increasing current density. A correlation similar to Peukert's equation [31] for lead–acid batteries has been found [12]:

$$\tau = \frac{K}{j^{\lambda}} \qquad (3)$$

where $\lambda = 1.27$ to 1.43.

Table 1 shows some numerical values demonstrating this feature. It can be seen that the potentiodynamic value is exceptionally low, which is due to the high current densities operating in this type of experiment.

Another parameter which governs the capacity of the synthesis electrode is given by the layer thickness of the electrode. The number of thermal activation cycles has been varied up to 50, corresponding to a layer thickness of about 10 μm. As was demonstrated formerly with the basic curve, μ was only 50% at thin layers and decreased to 20% for thicker ones [12]. This can be explained by our porous layer model. A similar behaviour is found in the presence of isopropanol, cf. Fig. 8 where bending of the curve is substantially diminished. The temperature of the firing step is another important parameter previously studied [11].

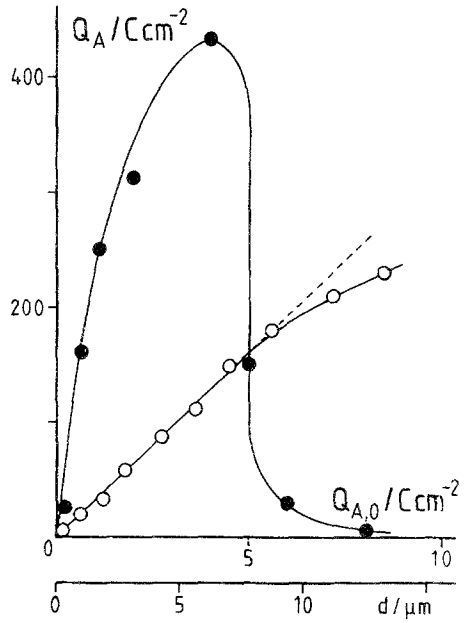

Fig. 8. Galvanostatic long-term behaviour in 1 M H_2SO_4/1 M isopropanol Q_A, Total charge up to passivation; $Q_{A,O}$, theoretical charge for $Cr_2O_3 \rightarrow 2CrO_3$. Variation of thickness of oxide layer with Z_a: O—O, binary system, chromium : titanium = 1 : 1.08, $j = 2.5\,mA\,cm^{-2}$ ●—●, ternary system, chromium : titanium : antimony = 1 : 1.08 : 0.92, $j = 10\,mA\,cm^{-2}$.

3.2.2. Ternary oxides. The service life of electrodes may be greatly improved by at least one order of magnitude by adding antimony oxide as a third component to the oxide system. The activation solution contained $SbCl_5$ (or $SbCl_3$) as a source of antimony, cf. section 2.1. No HCl addition was necessary to stabilize the solution. The mixture of oxides had a green-black to nearly black colour and adhered tightly to the titanium.

Current–voltage curves [12], exhibited a second peak at $U_S = 1.6$ V, which is ascribed to the oxidation Sb(III) → Sb(V). This means that $SbCl_5$ is transformed to Sb_2O_5, which decomposes thermally in the course of the firing step, cf. Section 3.1.

The influence of antimony concentration on the long-term stability of the electrode was investigated under galvanostatic conditions with anodic oxidation of isopropanol as the model reaction. As shown in Table 2, an optimum composition of chromium : titanium : antimony of about 2 : 1 : 1 (atomic ratio) was found. Doubling of the antimony concentration led to

Table 2. Dependence of service life of $Ti/Cr_2O_3/TiO_2$ standard ternary oxide anodes in 1 M H_2SO_4/1 M isopropanol on a third oxide component. Current density = 20 mA cm^{-2}

Oxide electrode	τ *(h)*	Q_A *(C cm^{-2})*	TOF_{pract} *($Q_{A,O}$ = 0.30 C cm^{-2})*
Cr:Ti (2:1.08)	0.14	10.4	34
Cr:Ti:Sb (2:1.08:0.25)	0.17	12	40
Cr:Ti:Sb (2:1.08:0.50)	1.43	103	344
Cr:Ti:Sb (2:1.08:0.92)	1.78	128	416
Cr:Ti:Sb (2:1.08:1.3)	1.69	121	404
Cr:Ti:Sb (2:1.08:2)	0.5	36	120
Cr:Ti:Sn (2:1:1)	0.13	9	30
Cr:Ti:Ag (2:1:0.5)[a]	0.17	3	10
Cr:Ti:Au (2:1:0.54)	0.033	2.4	8

[a] Chromium and silver as nitrates; j = 5 mA cm^{-2}.

a strong decay of service life. Table 2 contains, in addition, the results of three other ternary systems with tin, silver or gold as the third component. In spite of the fact that tin greatly stabilizes chlorine anodes based on RuO_2/TiO_2 [32], no improvement was found in the case of Cr_2O_3 anodes.

Galvanostatic runs in 1 M H_2SO_4/1 M isopropanol up to depletion of chromium, indicated by a rise of potential, were performed at various current densities. The results are shown on a double logarithmic plot in Fig. 9, confirming the relationship indicated by Equation 3. The exponent λ, which is given in the figure, seems to be somewhat higher than for the binary systems.

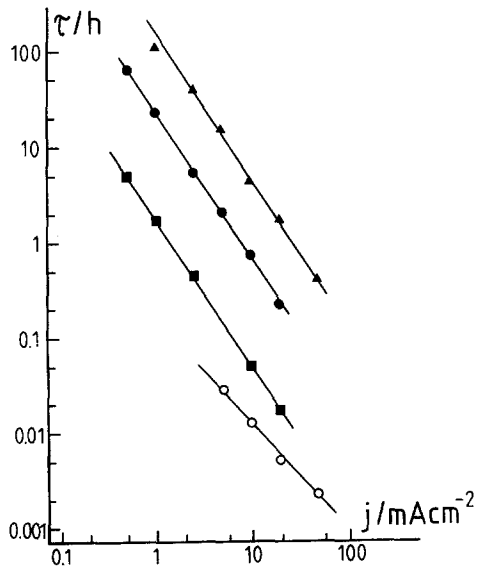

Fig. 9. Double logarithmic plot of galvanostatic life time, τ, for Ti/Cr_2O_3, TiO_2, Sb_2O_4 anodes, with chromium : titanium : antimony = 1 : 1.08 : 0.92 at various current densities, j. Electrolytes: o—o 1 M H_2SO_4, λ = −1.08; ▲—▲ 1 M H_2SO_4/1 M isopropanol, λ = −1.53; ●—● 1 M H_2SO_4/1 M tetrahydrofuran, λ = −1.52; ■—■ 1 M H_2SO_4/1 M methyl-β cyanoethyl ether; λ = −1.52.

Variation of Q_A with thickness of the ternary oxide layer led, at small layer thickness, to a curve resembling that of the binary system, cf. Fig. 8. However, thick layers showed a sharp collapse of long-term capacity. This phenomenon is correlated with detachment of the whole black oxide layer as a thin sheet, leaving behind the titanium metal virtually unchanged. The maximum corresponds to 430 C cm^{-2} or τ = 12 h at 10 mA cm^{-2}.

3.3. *Preparative results*

3.3.1. Isopropanol. Samples of 1 M isopropanol in 1 M H_2SO_4 were anodically oxidized in a quasi-divided cell (cf. Section 2.2) at constant current densities of j = 1 and 5 mA cm^{-2}. The anode, standard ternary oxide Ti/Cr_2O_3, TiO_2, Sb_2O_4, Cr : Ti : Sb = 1 : 1.08 : 0.92, had an area of 300 cm^2. Currents were therefore 0.3 and 1.5 A.

Table 3 shows the results of preparative long-term runs. Two electrodes, A and B, were used. These were prepared with three or five activation cycles. Conversion of isopropanol, calculated from the charge, was β = 20–60%. A virtual

Table 3. Preparative results for the anodic oxidation of isopropanol, 1 M H_2SO_4/1 M isopropanol, standard ternary oxide anode. Initial amount of isopropanol, 0.5 mol

Run	*Electrode*	j *(mA cm^{-2})*	Q *(A h)*	*β (% theor.)*	*Acetone (mol)*	*Current efficiency (%)*	*End potential (U_S/V)*
1	A	5	5.36	20	0.089	89	–
2	A	1	7.8	29.1	0.146	101	1.25
3	B	5	5.36	20	0.098	98	–
4	B	1	20.42	59	0.400[a]	105	1.50

[a] Initial amount of isopropanol, 650 mmol.

quantitative current efficiency for acetone was found in the last three runs. Acetone was the only product found in HPLC analysis.

The end potential of electrode B was U_S = 1.50 V, indicating a nearly total depletion of the chromium inventory which was 0.122 g chromium, corresponding to 0.45 g oxide mixture. From this we calculate a TOF_{pract} of 271 (cf. Section 4). This is 65% of the value given in Table 2, which was obtained with j = 20 mA cm^{-2}; it is only 15% with regard to the value which is obtained after correction with the aid of Equation 3 and Fig. 9 for an average current density of 2.5 mA cm^{-2}. It must be concluded that the spray method, used for the preparation of the larger electrodes, is somewhat inferior to the painting method for the small electrodes.

Electrode A had a weight loss of 0.0614 g after the two runs, corresponding to 0.81 mmol Cr_2O_3. From this we calculate a TOF of 202, which is only 11% of that value calculated from the small-scale tests for the same current density.

The quantitative current efficiencies found with these electrodes agree with a quantitative yield of acetone for the chemical oxidation of isopropanol [33]. Anodic oxidation with platinum electrodes leads to a current efficiency of only 70% [34]. Other products such as acetic acid, formic acid and CO_2 are found in this case. We conclude from this an exceptionally high selectivity of the Cr_2O_3 anode for this oxidation. The same Westheimer mechanism as in homogeneous solution [35, 36] is operative at the electrode surface (cf. Fig. 10). This is not only proved by the quantitative preparative result but also by additional, independent experimental arguments [13].

3.3.2. Tetrahydrofuran. The anodic oxidation of this cycloaliphatic ether is not very selective. As Table 4 shows, the products of a two-, four- and eight-electron oxidation in the α-position, i.e. 2-hydroxy-THF and γ-butyrolactone, besides their products of hydrolysis and succinic acid, respectively, have been found in comparable amounts. The current efficiency for butyrolactone was 53%. Similar results have been obtained with PbO_2 [37]. Recently, an excellent selectivity for the most interesting primary product, 2-hydroxy-THF, has been found at platinum anodes in 1 M H_2SO_4 [37]. The current efficiencies total 87%. The rest should be due to several low-boiling side products, which were not identified.

The primary attack of CrO_3 may be at the ether oxygen, as for RuO_4 as an oxidant which leads selectively to butyrolactone [38, 39], but more probably it is the α-methylene group that is attacked. The further sequence of reactions corresponds totally to Fig. 11, which will be

Table 4. Anodic oxidation of tetrahydrofuran (1 M THF, 1 M H_2SO_4) at a standard ternary oxide anode. j = 0.5 mA cm^{-2}; I = 0.15 A; Q = 46 A h, τ = 307 h; n_0 = 525 mmol

Product	*Electron number*	n_{prod} *(mmol)*	*Current efficiency (%)*
2-Hydroxy-THF	2	208	24
γ-Butyrolactone *and* γ-Hydroxy-butyric acid	4	226	53
Succinic acid	8	21	10

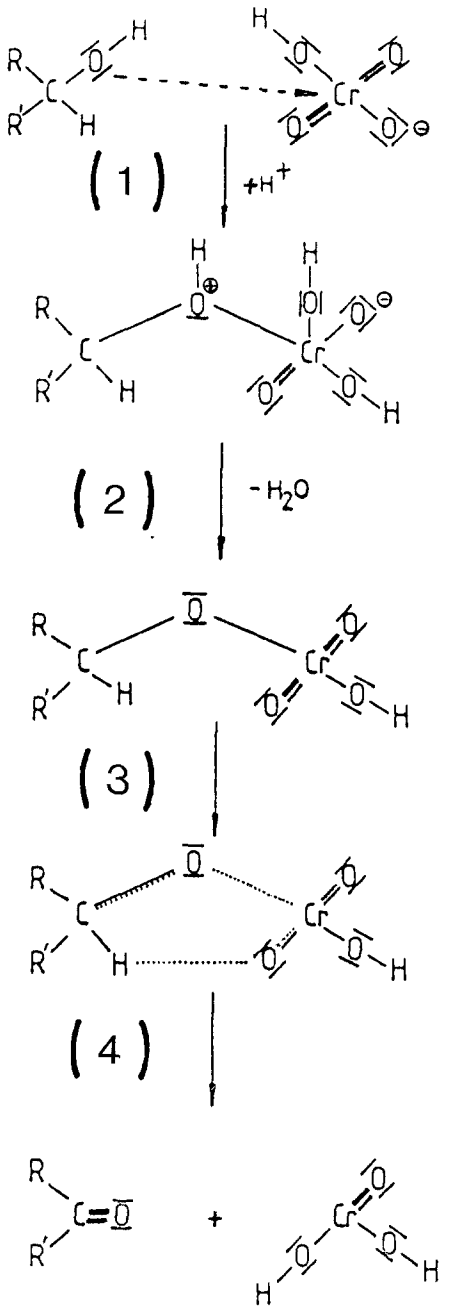

Fig. 10. Westheimer mechanism at the surface of a Ti/Cr_2O_3 anode for the oxidation of a secondary alcohol to a ketone, $HCrO_4^-$, is part of the electrode surface. (1) Complexation; (2) esterification; (3) cyclic complex, hydride shift; (4) product formation.

discussed in the next section. The formation of succinic acid starts from γ-hydroxy-butyric acid. The mechanisms of Figs 10 and 11 proceed successively at the $-CH_2OH-$ and the $-CHO-$ groups. In all these cases the characteristic five-membered cyclic transition state is accomplished.

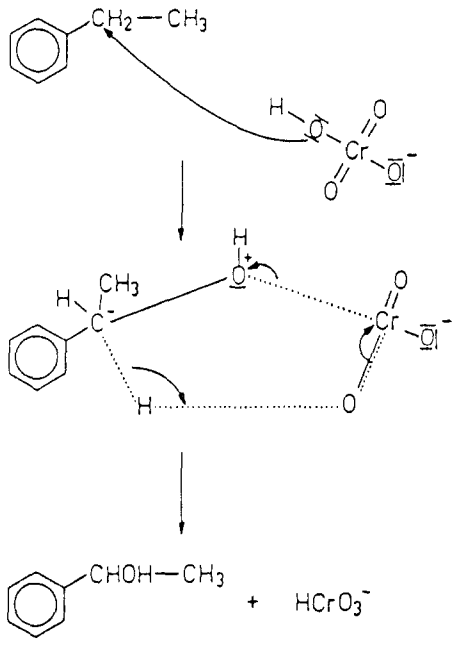

Fig. 11. Mechanism for the oxidation of ethylbenzene to 1-phenyl-ethanol with chromic acid.

3.3.3. Ethylbenzene. The last example is ethylbenzene, which was dissolved in 96 vol % acetonitrile at a concentration of 0.2 M. The electrolyte concentration was 1 M H_2SO_4. The low water concentration has a favourable effect on the service life of the electrode [12]. Table 5 gives the current efficiencies for two products in the course of an electrolysis with $j = 0.5\,mA\,cm^{-2}$.

Acetophenone was formed as the main product, but with relatively low current efficiency. As the current efficiency goes through a maximum, acetophenone must itself play a role as an intermediate. The same holds for benzaldehyde at a low current efficiency level. The identity of four further HPLC peaks ($MeOH/H_2O$ 3 : 1 as an eluent) could not be clarified. However, phenylacetic acid could be excluded as well as 1-phenylethanol and 2-phenylethanol. The presence of benzoic acid as a further product is probable. Benzaldehyde is known to be rapidly oxidized to benzoic acid with chromic acid [1]. Acetophenone is found to be the main product for the chemical oxidation of ethylbenzene with aqueous sodium chromate solution [40] and for the anodic oxidation at platinum [41]. At a PbO_2

Table 5. Electrolysis of 0.1 mol ethylbenzene at the standard ternary oxide anode. $j = 0.5\,mA\,cm^{-2}$; $I = 0.15\,A$

τ (h)	Q (A h)	Current efficiency for acetophenone (%)	Current efficiency for benzaldehyde (%)
24.1	3.6	19.5	–
30.1	4.5	20.0	1.4
44.8	6.7	15.6	1.0
70.2	10.5	11.4	0.9
93.6	14.0	9.5	–

anode the benzene ring underwent additional anodic attack and ethylquinone was found as a product [42]. Chromic acid oxidizes the aromatic ring only slowly.

The reactive centre of ethylbenzene is the methylene group [1, 2]. According to Fig. 11, chromic acid coordinates with this centre and again forms a five-membered ring as an intermediate. This dissociates into 1-phenylethanol and a Cr(VI) compound. An OH group from chromic acid is virtually transferred. The alcohol is further oxidized according to the Westheimer mechanism.

4. Concluding remarks

These results show clearly that heterogeneous redox catalysis is operative when ceramic composite anodes Ti/Cr_2O_3, TiO_2 (Sb_2O_4) are employed in the types of organic electrosynthesis given in Section 3. In the electrochemical step, Cr_2O_3 surface groups are oxidized,

$$(Cr_2O_3)_s + 3H_2O \xrightarrow{k_e} 2(CrO_3)_s + 6H^+ + 6e \tag{4}$$

where k_e is the electrochemical rate constant. The reaction mechanism branches thereafter; two chemical follow-up reactions compete in consuming $(CrO_3)_s$. One is the chemical reaction of the dissolved organic compound, rate constant k (cf. Equation 2). It finally regenerates (Cr_2O_3) or (CrO_2). The other reaction is the hydration which leads to the dissolution of CrO_3 as chromic acid, with a rate constant k_{dis} (cf. Equation 1). In the steady state, the following rate balance holds:

$$v_e = v + v_{dis} \tag{5}$$

After the passage of a charge Q_A, the chromium inventory is depleted. From this charge the following equation for the life time of the electrode has been derived [12]:

$$\tau = \mu z F (Cr_2O_3)_0 \left(1 + \frac{k}{k_{dis}}\right) \Big/ j \tag{6}$$

where $(Cr_2O_3)_0$ is the total inventory of chromium oxide at the electrode and μ is for a normal layer thickness of about 50%. Equation 6 can easily be rearranged to yield TOF_{pract}:

$$TOF_{pract} = \frac{\tau j}{\mu z F (Cr_2O_3)_0} = \frac{Q_A}{Q_{A,O(pract)}} = \left(1 + \frac{k}{k_{dis}}\right) \approx \frac{k}{k_{dis}} \tag{7}$$

From the ratio of the rate constants k for isopropanol oxidation and k_{dis}, determined independently, a value of 460 for TOF could be derived [14]. From the experimental values for Q_A and $Q_{A,O(pract)}$, a TOF_{pract} of 100 to 416 has been found, as demonstrated in this paper. For Cr_2O_3 on chromium (steel), no heterogeneous redox catalysis has been found [17].

The stability of the anodes should be further improved. One attractive method is by the introduction of stabilizing oxide or other inorganic additives. Low current densities improve Q_A substantially according to Equation 3. For practical applications, low current density is not ideal but not prohibitive, as is demonstrated by the successful industrial development of alcohol oxidation at nickel oxide anodes [43].

The problems with the stoichiometric application of chromic acid, stated in the Introduction, could be partially solved with our anodes, which give

(i) much lower chromium inventory,

(ii) no toxicity hazards, handling only with chromium (III),

(iii) separation of much lower amounts of dissolved Cr(III),

(iv) recycling *on* the electrode up to 400 times.

Acknowledgements

Financial support of this work by Deutsche Forschungsgemeinschaft is gratefully acknowledged. Auger electron spectroscopy by Dr. Hantsche, BAM, Berlin (Fig. 3), and SEM (ED) by Dr Ströder, Heraeus Co., Hanau (Fig. 2), is gratefully appreciated. We are indebted to Thyssen Edelstahl AG, Krefeld, for generous provision of titanium sheet Contimet 35.

References

[1] K. B. Wiberg, Oxidation in Organic Chemistry, Academic Press, New York (1965).
[2] D. L. Lee, in 'Oxidation', Vol. 1 (edited by R. L. Augustine), Marcel Dekker, New York (1971) chapter 1.
[3] L. J. Chinn, 'Selection of Oxidants in Synthesis', Marcel Dekker, New York (1971).
[4] L. F. Fieser and M. Fieser, 'Reagents for Organic Synthesis', Vol. 1 (1967) to Vol. 11 (1984), John Wiley and Sons, New York.
[5] G. Cainelli and G. Cardillo, 'Chromium Oxidations in Organic Chemistry', Springer-Verlag, Berlin (1984).
[6] R. F. Gross and A. Hickling, *J. Chem. Soc.* (1937) 325.
[7] M. Käppel, *Chem. Ing. Techn.* **35** (1963) 386.
[8] R. Clarke, A. T. Kuhn and E. Okoh, *Chem. in Britain* **11** (1975) 59.
[9] W. Breckheimer and R. Schütze, *Z. Elektrochem.* **57** (1953) 857.
[10] Germ. Pat. 109012 (1897), 117949 (1899), C. F. Darmstädter, cf. F. Fichter, 'Organische Elektrochemie', Th. Steinkopff, Dresden (1942) p. 13.
[11] F. Beck and H. Schulz. *Ber. Bunsenges. Phys. Chem.* **88** (1984) 155.
[12] *Idem, Electrochim. Acta* **29** (1984) 1569.
[13] H. Schulz and F. Beck, *Angew. Chem. Int. Ed. Engl.* **24** (1985) 1049.
[14] F. Beck, W. Gabriel and H. Schulz, *DECHEMA Monograph.* **102** (1986) 339.
[15] H. B. Beer, DDR-Pat. 55223 (1965).
[16] *Idem,* Belg. Pat. 710551 (1967).
[17] F. Beck, H. Schulz, B. Jansen, *Electrochim. Acta* **31** (1986) 1131.
[18] F. Beck and E. Zimmer, unpublished results.
[19] H. Schulz, PhD thesis, University of Duisburg (1985).
[20] B. Wermeckes and F. Beck, *Chem. Ber.* **118** (1985) 3771.
[21] *Idem, Electrochim. Acta* **30** (1985) 1491.
[22] O. Glemser, U. Hauschild and F. Trüpel, *Z. anorg. allg. Chem.* **277** (1954) 113.
[23] R. S. Schwarz, I. Fankuchen and R. Ward, *J. Amer. Chem. Soc.* **74** (1952) 1676.
[24] F. Beck and W. Gabriel, *Angew. Chem. Int. Ed. Engl.* **24** (1985) 771.
[25] E. Schwarzmann, 'Hydroxide, Oxidhydrate und Oxide', Steinkopff-Verlag, Darmstadt (1976).
[26] W. Mayer, *Z. Phys.* **85** (1933) 278.
[27] *Idem, Z. Elektrochem.* **50** (1944) 274.
[28] K. Hauffe and J. Block, *Z. Phys. Chem.* **198** (1951) 232.
[29] P. R. Chapman, R. H. Griffith and J. D. F. Marsh, *Proc. R. Soc. A* **224** (1954) 419.
[30] F. Beck, H. Schulz, to be published.
[31] F. Beck, *J. Electrochem. Soc.* **129** (1982) 1880.
[32] US-Pat 3776834 (8/73, Diamond Shamrock, c/o K. J. O'Leary), cf. Germ. Off. 2342663.
[33] F. H. Westheimer and A. Novick, *J. Chem. Phys.* **11** (1943) 506.
[34] K. Elbs and O. Brunner, *Z. Elektrochem.* **6** (1900) 609.
[35] F. H. Westheimer, *Chem. Rev.* **45** (1949) 419.
[36] F. H. Westheimer and N. Nicolaides, *J. Amer. Chem. Soc.* **71** (1949) 25.
[37] F. Beck, B. Wermeckes and H. Schulz, *Tetrahedron* **43** (1987) 577.
[38] D. G. Lee and M. van den Engh, *Can. J. Chem.* **50** (1972) 3129.
[39] L. M. Berkowitz and P. N. Rylander, *J. Amer. Chem. Soc.* **80** (1958) 6682.
[40] D. G. Lee and U. A. Spitzer, *J. Org. Chem.* **34** (1969) 1493.
[41] E. J. Krynchkova, A. V. Solomin and M. I. Usanovich, *Elektrokhimiya* **8** (1972) 116; English translation p. 113.
[42] Kashichi Ono, *Helv. Chim. Acta* **10** (1927) 45.
[43] P. Seiler and P. M. Robertson, *Chimia* **36** (1982) 305.